AD-A188 461 OPTICAL SIGNAL PROCESSING USING NONLINEAR OPTICS(U) 1/1
UNIVERSITY OF SOUTHERN CALIFORNIA LOS ANGELES DEPT OF
ELECTRI W H STEIER 1987 AFOSR-TR-87-6689
UNCLASSIFIED AFOSR-84-0207 F/G 20/6 NL

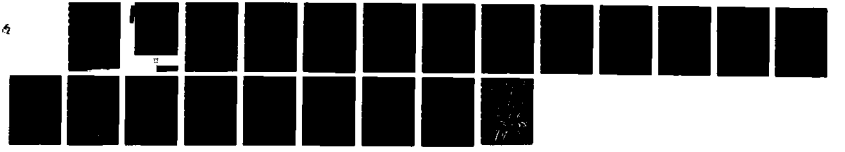

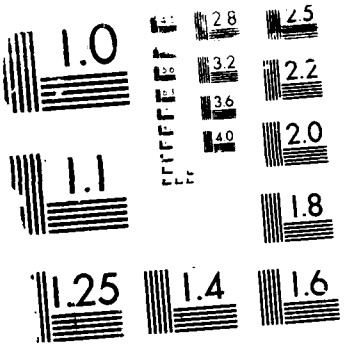

MICROCOPY RESOLUTION TEST CHART

(2)

UNIVERSITY OF SOUTHERN CALIFORNIA
SCHOOL OF ENGINEERING

AFOSR-TR- 87-1689

OPTICAL SIGNAL PROCESSING USING NONLINEAR OPTICS

Grant AFOSR-84-0207

FINAL REPORT

For the Period
August 1, 1984 - September 31, 1987

presented to:

Air Force Office of Scientific Research
Building 410
Bolling Air Force Base, D.C. 20332

presented by:

William H. Steier
Eletrical Engineering/Electrophysics
University of Southern California
Los Angeles, CA 90089-0483

SECURITY CLASSIFICATION OF THIS PAGE

REPORT DOCUMENTATION PAGE

1a REPORT SECURITY CLASSIFICATION UNCLASSIFIED	1b RESTRICTIVE MARKINGS
2a SECURITY CLASSIFICATION AUTHORITY	3 DISTRIBUTION / AVAILABILITY OF REPORT
2b DECLASSIFICATION / DOWNGRADING SCHEDULE	Approved for public release, distribution unlimited
4 PERFORMING ORGANIZATION REPORT NUMBER(S)	5 MONITORING ORGANIZATION REPORT NUMBER(S) AFOSR-TR- 87-1689

6a NAME OF PERFORMING ORGANIZATION: University of So. California	6b OFFICE SYMBOL (If applicable)	7a NAME OF MONITORING ORGANIZATION: AFOSR	
6c ADDRESS (City, State, and ZIP Code): Electrical Engineering/Electrophysics, Los Angeles, CA 90089-0483		7b ADDRESS (City, State, and ZIP Code): Bldg 410, Bolling AFB, DC 20332-6448	
8a NAME OF FUNDING / SPONSORING ORGANIZATION: SAME AS 7 a	8b OFFICE SYMBOL (If applicable)	9 PROCUREMENT INSTRUMENT IDENTIFICATION NUMBER: AFOSR-84-0207	
8c ADDRESS (City, State, and ZIP Code): SAME AS 7b		10 SOURCE OF FUNDING NUMBERS	
		PROGRAM ELEMENT NO: 61102F	PROJECT NO: 2305
		TASK NO: B4	WORK UNIT ACCESSION NO:

11 TITLE (Include Security Classification)
Optical Signal Processing Using Nonlinear Optics

12 PERSONAL AUTHOR(S)
William H Steier

13a TYPE OF REPORT: Final Report	13b TIME COVERED: FROM 01 Aug 84 TO 31 Sep 87	14 DATE OF REPORT (Year, Month, Day)	15 PAGE COUNT

16 SUPPLEMENTARY NOTATION

17 COSATI CODES			18 SUBJECT TERMS (Continue on reverse if necessary and identify by block number)
FIELD	GROUP	SUB-GROUP	

19 ABSTRACT (Continue on reverse if necessary and identify by block number)

The 2-D correlation/convolution which can be achieved in real time via four wave mixing in nonlinear materials has been investigated in detailed to determine the accuracy and signal power possible. This analysis was initiated under other support; the experimental confirmation was completed under this contract. The analysis which is based on Fourier transforms of the equations nonlinear interactions has resulted in a closed from solution for the output and clearly shows how it differs from the desired 2-D correlation. In the example of a scene that is searched for given objects, the accuracy decreases as the ratio of scene to object size increases. The accuracy also decreases as the length of the nonlinear material increase resulting in a trade-off between accuracy, size of the scanned scene, and power signal to noise ratio in the output.

20 DISTRIBUTION / AVAILABILITY OF ABSTRACT ☐ UNCLASSIFIED/UNLIMITED ☐ SAME AS RPT ☐ DTIC USERS	21 ABSTRACT SECURITY CLASSIFICATION UNCLASSIFIED	
22a NAME OF RESPONSIBLE INDIVIDUAL: DR C LEE GILES	22b TELEPHONE (Include Area Code): (202) 767-4931	22c OFFICE SYMBOL: NE

DD FORM 1473, 84 MAR — 83 APR edition may be used until exhausted. All other editions are obsolete.

SECURITY CLASSIFICATION OF THIS PAGE

OPTICAL SIGNAL PROCESSING USING NONLINEAR OPTICS

FINAL REPORT

For the Period August 1, 1984 - September 31, 1987

Introduction:

This report summarizes the results obtained on Grant AFOSR-84-0207, "Optical Signal Processing using Nonlinear Optics", for the period 8/1/84-7/31/87.

2-D Correlations/Convolutions via Four Wave Mixing:

The 2-D correlation/convolution which can be achieved in real time via four wave mixing in nonlinear materials has been investigated in detail to determine the accuracy and signal power possible. This analysis was initiated under other support; the experimental confirmation was completed under this contract. The analysis which is based on Fourier transforms of the equations of nonlinear interactions has resulted in a closed from solution for the output and clearly shows how it differs from the desired 2-D correlation. In the example of a scene that is searched for given objects, the accuracy decreases as the ratio of scene to object size increases. The accuracy also decreases as the length of the nonlinear material increases resulting in a trade-off between accuracy, size of the scanned scene, and power or signal to noise ratio in the output.

The first result of this analysis is the realization that a non-colinear interaction is considerably less accurate than a colinear. In the typical four-wave mixing scheme, the two inputs, B_1 and B_2, propagate at a small angle to each other within a nonlinear medium; the pump wave is counter to one of the inputs. This angle between the beams results in a lateral translation between the patterns as they propagate through the nonlinear material. The result is a correlation between smoothed versions of the inputs and a considerable error.

A colinear interaction is possible so long as the two inputs are

distinguished via either polarization or wavelength. A typical polarization scheme is shown in Figure 1. Input 2 interacts with the plane wave pump 3 to write a grating in the nonlinear material. Input 1 reads the grating and results in the scattered output 4. Note that a true χ_3 material such as CS_2 will not work in all cases since the output will contain the correlation and its complex conjugate. If the inputs are real, this is not objectionable.

The result for the colinear cases is:

$$B_4(x,y) = K_c \int_{-\infty}^{+\infty} dx'dy' B_1(x',y') B_2(x'+x,y'+y) \frac{1-\exp(i\gamma_c z_o)}{-1\gamma_c z_o}$$

where

$$\gamma_c = i\alpha \frac{k_0}{nF^2} (xx'+yy')$$

K_c	=	constant containing the nonlinear coefficient χ_3
z_o	=	thickness of nonlinear material
α	=	linear loss coefficient
F	=	Focal length of the F.T. lens

The above expression differs from the desired 2-D correlation by the last bracketed term containing the exponent. The origin of this term is the k vector mismatch. Near the origin, the correlation is relatively accurate, but the accuracy decreases as the size of the two input patterns increase. This is important in a typical case where a scene is scanned for a particular object. For large fields of scan, the accuracy decreases, and the possibility of false alarms increases.

This analysis has been confirmed by an experiment which was performed under the support of this grant. In the experiment, input 1 is a square aperture of side "a" located on the axis. Input 2 is similar square aperture but located X_o off axis. We are, therefore, searching over range 2Xo by 2Xo for the square

aperture of side "a". In the experiment, the relative correlation power (RCP) was measured and compared to the calculated value. The RCP is the ratio of the total integrated power in the correlation peak, relative to the power in the perfect correlation and is, therefore, the relative detected power for the threshold detection scheme.

The experimental layout is shown in Figure 2. C is the photorefractive material bismuth silicon oxide which is oriented so that the beams propagated along the 001 direction. The half wave plate H_1 rotates the polarization of the write beam $B_2(x,y)$ to be perpendicular to that of the read beam $B_1(x,y)$. The mask I contains on on-axis rectangular aperture which is illuminated by B1 and three off-axis rectangular apertures illuminated by B_2. Three correlations are thus recorded simultaneously for accuracy. The slit on the chopper (Ch) wheel selected one of the correlations at a time for measurement by the PMT.

Typical comparison of the experimental data (crosses and dashed line) and the calculated data is shown in Figure 3. The parameters c, d, and b are defined on the figures and earlier in this report. The results closely follow the predicted curve and confirm the analysis. The results are presented in Publication 1.

Measurement of the Photorefractive Properties of GaAs

GaAs is a fast photorefractive material that can be used in the infrared where diode laser sources are available, and it is potentially fast because of its high electron mobility.[1-3] Nonlinear optical devices using GaAs can potentially be integrated with other opto-electronic devices which are also fabricated in GaAs.

D.C. Field Enhanced

To evaluate the potential of this material for infrared switching, we have made a series of measurements at 1.06μm, of the grating formation time and the two beam coupling gain as a function of intensity, grating wavelength, and applied voltage. The GaAs sample has a chrome concentration of $10^{17}cm^{-3}$,

dark resistivity of ~300 Megohm cm, and dimensions 10 mm x 10 mm x 5.5 mm. The applied electric field and the polarization vector were along the [111] direction. The inverse of the grating formation time varies linearly with intensity in accordance with theoretical predictions. For an incident laser intensity of 35 mW/cm^2, the grating formation time is 1.5 msec and increases to 1.8 msec on application of 6 kV. The gain increases with intensity and saturates. The saturated gain and the intensity required for saturation both increase with applied voltage. A maximum gain of 0.5 cm^{-1} at a grating spacing of 0.9μm was measured with no voltage applied which leads to a trap concentration of 10^{15} cm^{-3}. An applied voltage of 6 kV yielded a maximum gain of 0.9 cm^{-1} at a grating spacing of 1.2μm. It was observed that reducing the intensity decreases the gain and, at the same time, shifts the maxima of the gain curves to higher values of grating spacing both with and without an applied voltage. See Publication 2 for details.

A.C. Field Enhanced

The application of a.c. and step like fields was first proposed by Stepanov and Petrov.[4] We have obtained experimental data on the r.f. field enhanced gain as a function of the grating spacing for several r.m.s. electric fields at 7.7MHz. We find that application of r.f. fields has certain novel features when compared to the d.c. field case. The two beam coupling gain with applied r.f. field is insensitive to shadowing effects near the electrode and to non-uniform illumination. The entire applied r.f. field is sensed by the light beam in the crystal. The two beam coupling signal with applied r.f. field is also characterized by considerable stability when compared to signals obtained with applied d.c. fields. This stability of the signal is due to the fact that the space charge field in the r.f. case is totally imaginary; and the situation, except for the enhanced gain, is very much like the case when no field is applied. Lastly, the two beam coupling gain with applied r.f. fields is much larger for large grating spacing than the d.c. case. Typical results are shown in Figure 4.

We have derived an expression, based on the Kukhtarev equations, for two beam coupling gain with r.f. fields. A fit of the experimental data to the

predicted values yields a value of γ/μ for our sample where γ is the recombination coefficient and μ the mobility of the sample. Knowing the Debye length for our sample, we can calculate the diffusion length to be 0.3μ. See Publications 3 and 4 for details.

Enhancement by "Moving Grating"

It has been demonstrated in several photorefractive materials that a combination of an applied d.c. electric field and the "moving grating" technique can lead to enhanced two wave mixing gain. Two wave mixing gain depends upon the component of the index grating which is spatially shifted from the intensity interference pattern by 90° Applied d.c. electric fields can increase the magnitude of the index grating by drift but decreases the spatial phase shift. If this intensity interference pattern can be made to move with the correct velocity, the index grating can be resonantly enhanced. The interference pattern is made to move with constant velocity by a slight frequency shift in one of the recording beams.

The theoretical aspects of the "moving grating" technique have been discussed by Refregier[6] et.al., and Valley[5] has derived expressions and has predicted large gains for GaAs.

Figures 5 and 6 show the experimentally measured gain as a function of the grating wavelength for two values of the applied d.c. voltage (2kv and 4kv). The measured gains fit the theory only for an effective value of field less than the applied field, which is typical for d.c. field cases. In these measurements, the observed gain was optimized by adjusting the magnitude and frequency of the ramp voltage driving the transducer which moves one of the mirrors. The error bars on the data show the spread over several repeated measurements. For these measurements the strong beam intensity at the entrance face of the GaAs was held at 17 mW/cm^2.

The important material parameter in the theory of Valley is the ratio τ_{di}/τ_2. Where τ_{di} is the dielectric relaxation time and τ_2 is the inverse of the sum

of the photoproduction rate and the ion-recombination rate. Valley[5] shows that this ratio can be expressed as:

$$\frac{\tau_{di}}{\tau_2} = \frac{\varepsilon \gamma_R}{e\mu}$$

where γ_R is the electron recombination coefficient, ε is the dielectric constant, μ is the electron mobility, and e is the electron charge. The uncertainty is in the knowledge of γ_R/μ. Valley used values of μ=5800cm2/Vsec and γ_R=2.2x10^{-8} cm3/sec taken from the literature for GaAs samples with EL2 centers. Using these values, the predicted gains are considerably higher than those measured here, and the peak is shifted to longer grating wavelengths.

By measuring the enhanced two wave gain using r.f. electric fields in our sample, which is chrome doped, we found that the ratio of $\tau_{di}/\tau_2 = 0.25$ best fits that data. In these measurements, the uncertainty of the electric fields in the illuminated regions of the sample is not a problem. This value of τ_{di}/τ_2 was used for the theoretical curves of Figures 5 and 6. On the Figures are two theoretical curves; one for the electric field obtained by dividing the applied voltage by the electrode spacing, and one curve for the electric field which best fits the data. This discrepancy is typically seen in measurements of photorefraction because of the uncertainty of the electric field in the illuminated region of the material. The drop in the material resistivity in the illuminated regions decreases the fields in these regions. Even though an IR beam which filled the sample was used, there is unavoidable shadowing near the electrodes. Measurement of the d.c. field inside the crystal using the electro-optic effect yielded values as low as half the applied voltage. See Publication 6 for details.

Enhanced Opto-optical Light Deflection using Cavity Resonance

Dynamic opto-optical beam steering has been reported in several photorefractive materials[7,8]. In these switches, a grating is written by two optical control beams to steer or deflect an optical signal beam. Arrays of these

switches are essentially real time holograms, and they have potential use in dynamic optical interconnects for optical computing and in optical network switching. The efficiency, ν, (ν = % of the input beam that is deflected) of these switches is typically only a few percent for materials with reasonably fast response times. One approach to increasing the efficiency is to go to very long grating wavelengths and very high electric fields. Herriau, et.al.,[9] reported 95% efficiency in BGO at 20μm grating wavelength and 14Kv/cm applied field. We present here another technique that can potentially enhance the efficiency by an order of magnitude or more by using the grating to couple into a resonant cavity. This is similar in concept to the resonated holograms discussed by Collins[10].

Linear Cavity

Figure 7 shows the linear cavity configuration. The control beams at λ_c write a grating in the nonlinear material. The input beam (λ_s) is at Bragg angle for the grating. A portion of the input is deflected into the cavity which is resonant at λ_s. The light coupled through one of the mirrors is the output of the switch. Blocking a control beam will erase the grating and turn off the switch. The surfaces of the nonlinear material are set at Brewsters angle to minimize reflection losses in the resonator.

The efficiency of the combined grating and cavity can be more than an order of magnitude larger than ν if the cavity losses can be kept low. The rise and decay times of the switch will be increased by the cavity rise time; but for modest grating writing speeds, this should not be a factor. The bandwidth of the channel being switched will be reduced to the width of the cavity resonance. The greatest practical difficulty is keeping the cavity resonant at λ_s.

We have derived expressions for the switched power, the transmitted power, and the reflected power which are given in Publication 7. To demonstrate the concept, we have completed an experiment using $LiNbO_3$:Fe. The gratings were written at 4880Å and read at 6328Å. Using a grating with a measured 1.5% diffraction efficiency, the measured efficiency of the combined cavity and grating was 7.5%; a factor of 4.8 enhancement. This agreed well

with the theory using the measured cavity losses. The details are given in Publication 7.

Ring Cavity

The ring cavity, shown in Figure 8, has advantages over the linear cavity since no power is reflected back at the input and the circulating mode sees the loss and scattering of the $LiNbO_3$ only once per round trip. The disadvantage is the added scattering and absorption loss of the third mirror. Using a similar approach as the linear cavity, we have derived expressions for the efficiency of the ring cavity. In a demonstration experiment, the grating had a measured 2.3% diffraction efficiency at 6328Å. The cavity-grating combination had a measured diffraction efficiency of 12.8 % for a factor of 5.6 enhancement.

From the observed cavity resonance width, the round trip loss was measured and the theory was used to predict a 13.1% diffraction efficiency of the cavity-grating combination. See Publication 7 for more details.

References

1. M.B. Klein, Optics Letters, **9**, 350 (1984).

2. A.M. Glass, A.M. Johnson, D.H. Olson, W. Simpson, and A.A. Ballman, Appl. Phys. Letters, **44**, 948 (1984).

3. G. Albanese, J. Kumar, and W.H. Steier, Optics Letters, **11**, 650 (1986).

4. S. I. Stepanov and M.P. Petrov, Optics Comm., **53**, 292 (1985).

5. G.C. Valley, J. Opt. Soc. Am. B. **1**, 868 (1984).

6. P. Refregier, L. Solymar, H. Rajbenbach, and J.P. Huignard, J. Appl. Phys., **58**, 45 (1985).

7. A. Marrakchi, J.P. Huignard, and P. Gunter, Appl. Phys., **24**, 131 (1981).

8. E. Voit, C. Zaldo, and P. Gunter, Optics Lett., **11**, (5) 309 (1986).

9. J.P. Herriau, D. Rojas, J.P. Huignard, J.M. Bassat, and J.C. Launay, Ferroelectronics, **66**, 1 (1986).

10. S.A. Collins, OSA Topical Meeting on Optical Computer, Paper ME5, (1987).

Publications and Presentations of Research Results

Publications

1. Christopher Sexton and W. H. Steier, "The Accuracy of Real Time Correlations via Degenerate Optical Four Wave Mixing". CLEO '83, Baltimore, May 17-20, 1983, Paper TUB4.

2. G. Albanese, J. Kumar, and W.H. Steier, "Investigations of Photorefractive Behavior of Chrome-doped GaAs by using Alternating Electric Fields," Optics Lett., **11**, 650 (1986).

3. J. Kumar, G. Albanese, W.H. Steier, and M. Ziari, "Enhanced Two Beam Mixing Gain in Photorefractive GaAs using Alternating Electric Fields," Optics Lett., **12**, 120 (1987).

4. J. Kumar, G. Albanese, W.H. Steier, "Enhancement of Photorefractive Two Beam Coupling Gain by Radio Frequency Fields: Theory and Experiment," to appear JOSA-B, July, 1987.

5. J. Kumar, G. Albanese, and W.H. Steier, "Photorefractive Two Beam Coupling in GaAs:Cr with Applied r.f. Fields and Moving Gratings," Presented CLEO, Baltimore, MD., Paper WP2 April 1987.

6. J. Kumar, G. Albanese, and W.H. Steier, "Measurement of Two-wave Mixing Gain in GaAs with a Moving Grating," Optics Comm., **63**, 191 (1987).

7. W.H. Steier, G.T. Kavounas, R.T. Sahara, and J. Kumar, "Enhanced Opto-Optical Light Deflection using Cavity Resonance" submitted to Applied Optics.

8. G. Kavounas and W.H. Steier "Fast Hologram Erasure in Photorefractive Materials," to be presented OSA Topical Meeting on Photorefractive Materials, Effects, and Devices, UCLA, August, 1987.

Invited Presentations

1. "Opto-optical Switching," Lasers '86, Orlando, Florida, November 3 - 7, 1986.

- Collinear, degenerate FWM using orthogonal polarizations:

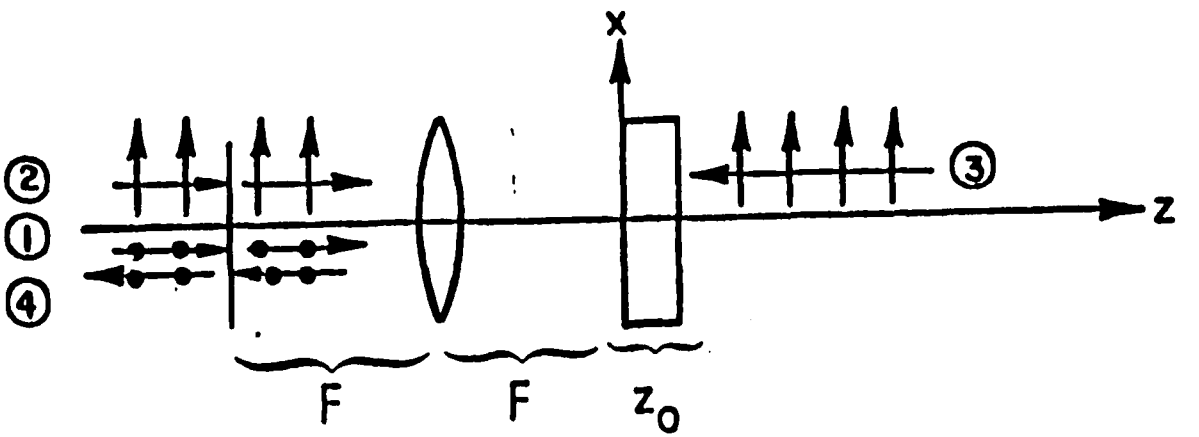

- ② and ③ write a grating, ① reads it
- Can't use a true $\chi^{(3)}$ material (e.g., CS_2)
- Strong noise at the input/output plane

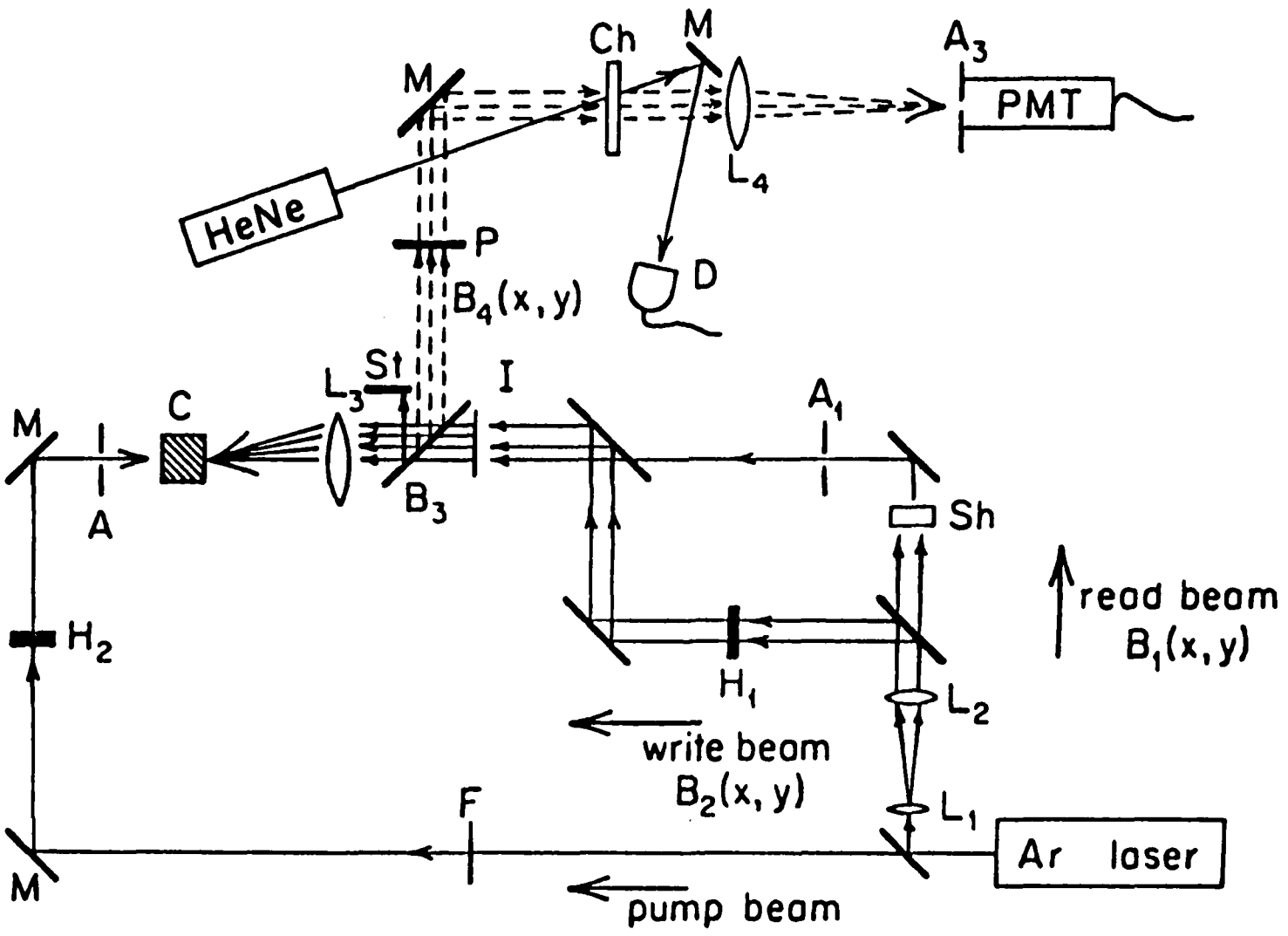

Figure 2 Experimental layout for observing 2-D correlations.

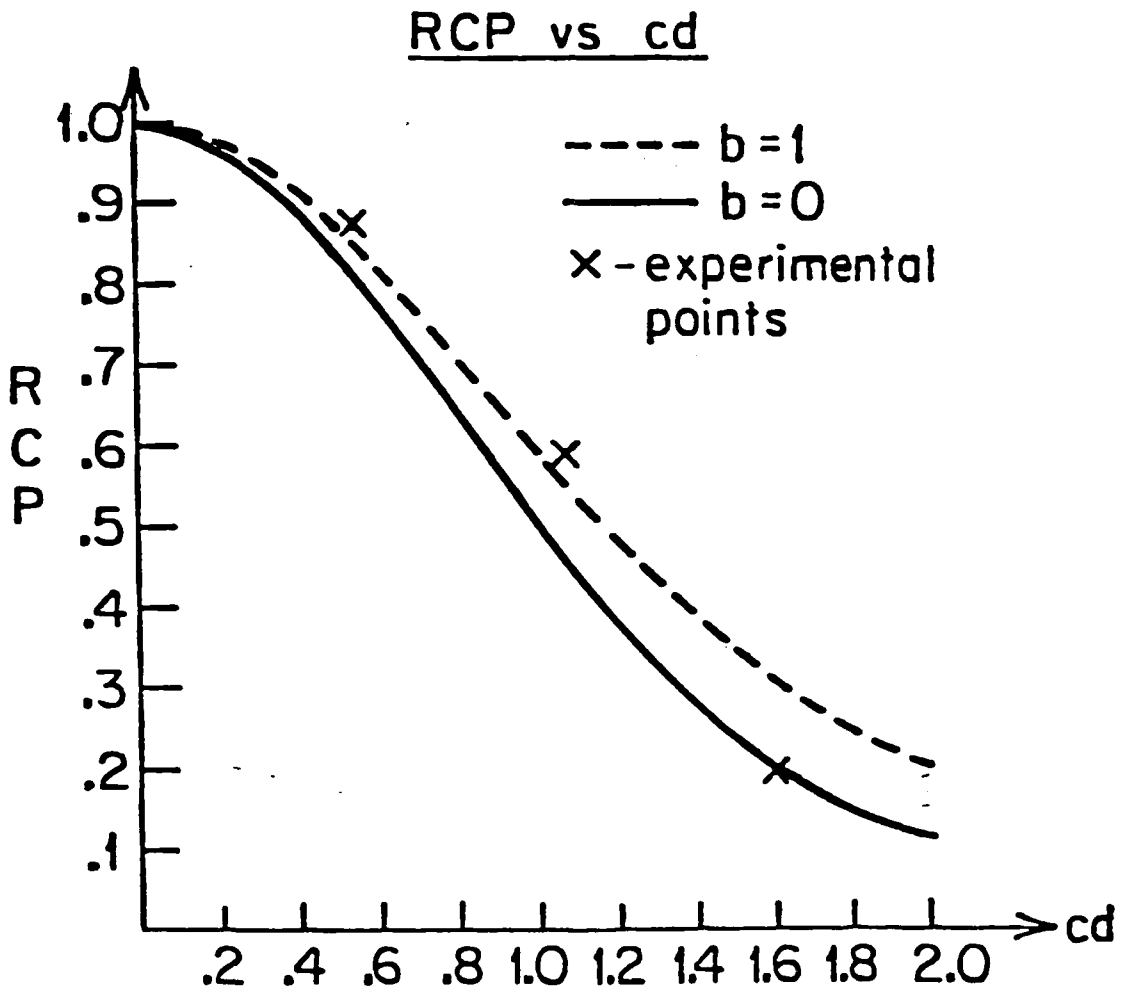

$$\left(c = \frac{z_0 a^2}{h\lambda F^2};\quad d = \frac{x_0}{a};\quad b = \alpha z_0\right)$$

$$cd = \frac{z_0 a x_0}{h\lambda F^2}$$

Figure 3. Relative correlations power (RCP) as a function of the interaction length. See text for definition of the parameters.

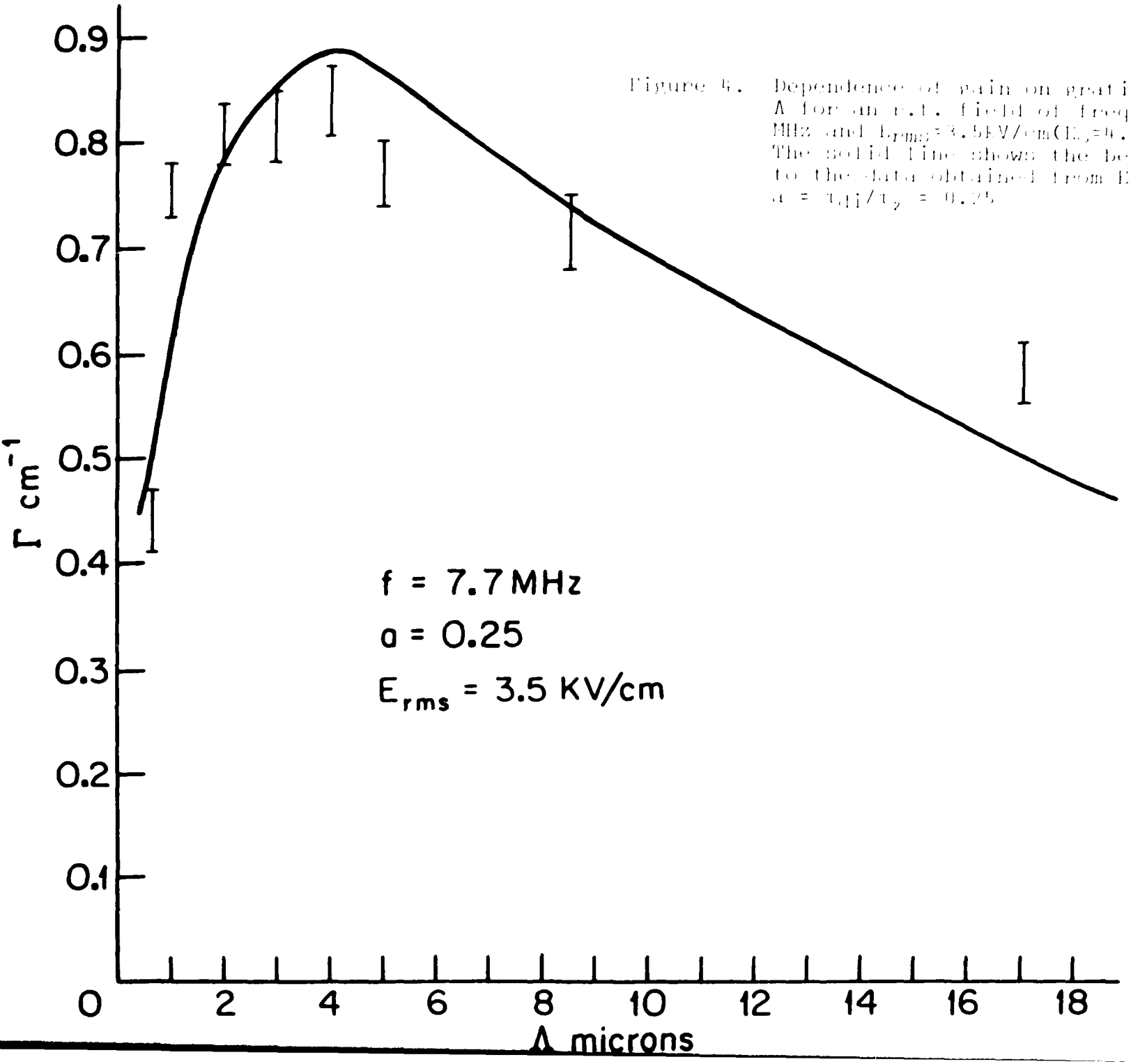

Figure 5. Dependence of gain on grating spacing Λ for an r.f. field of frequency 7.7 MHz and E_{rms}=3.5kV/cm(E_0=4.9kV/cm). The solid line shows the best fit to the data obtained from Eq. $a = \tau_{ji}/\tau_g = 0.25$

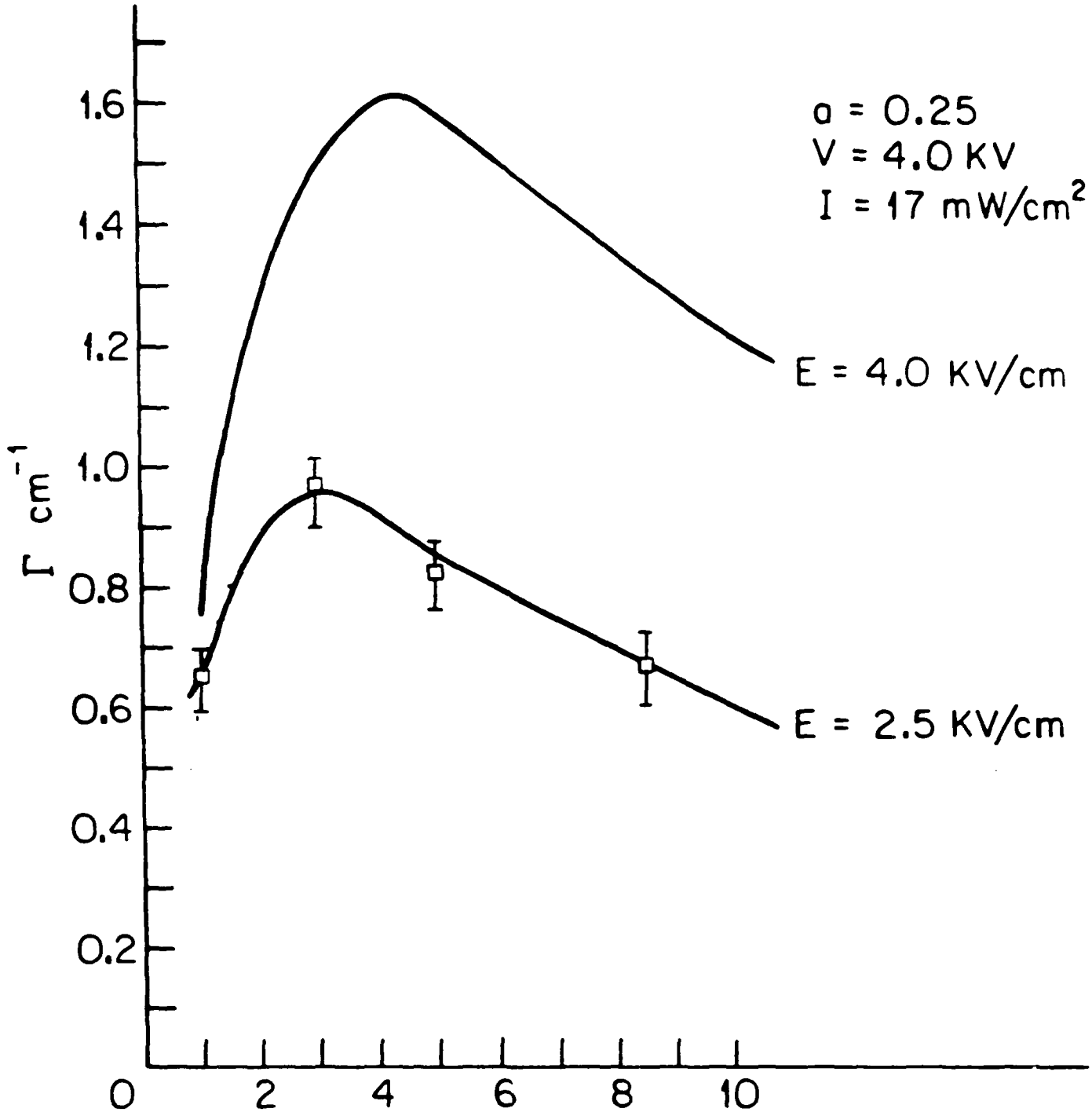

Figure 5. Two wave mixing gain, Γ, as a function of grating wavelength, Λ, for the moving grating case when the voltage applied across the sample was 2Kv. The square dots with error bars are the experimental data. Two solid theoretical curves are shown both using the parameter $a = \tau_{di}/\tau_2 = 0.25$ which was earlier found appropriate for the GaAs sample. The upper theoretical curve is for an electric field found by dividing the applied voltage by the crystal width. The second curve is for an electric field which best fits the data.

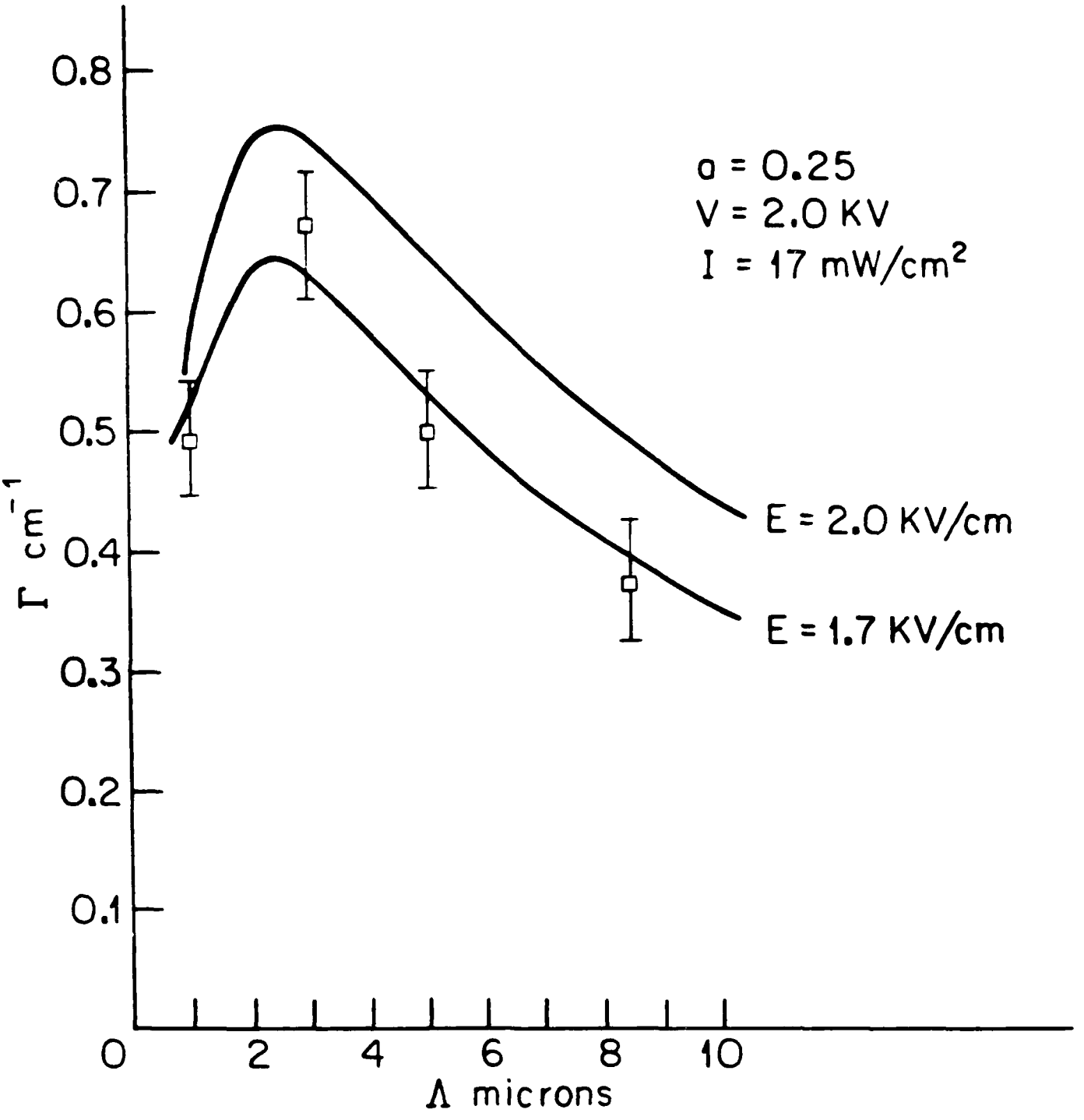

Figure 6. Two wave mixing gain, Γ, as a function of grating wavelength, Λ, for the moving grating case when the voltage applied across the same moving grating case was 4kV. See the caption of Figure 5 for an explanation of the two solid theoretical curves.

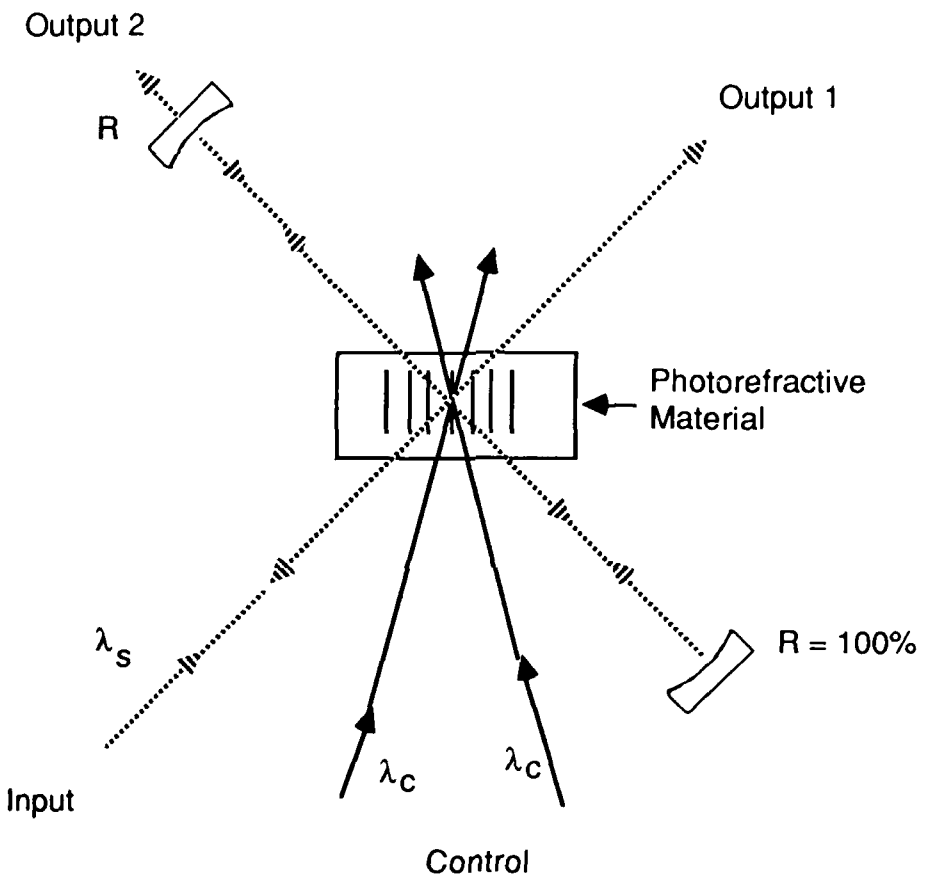

Figure 7. Enhanced opto-optical light deflection using a linear cavity. The dashed lines are the signal beam; the solid lines are control beams.

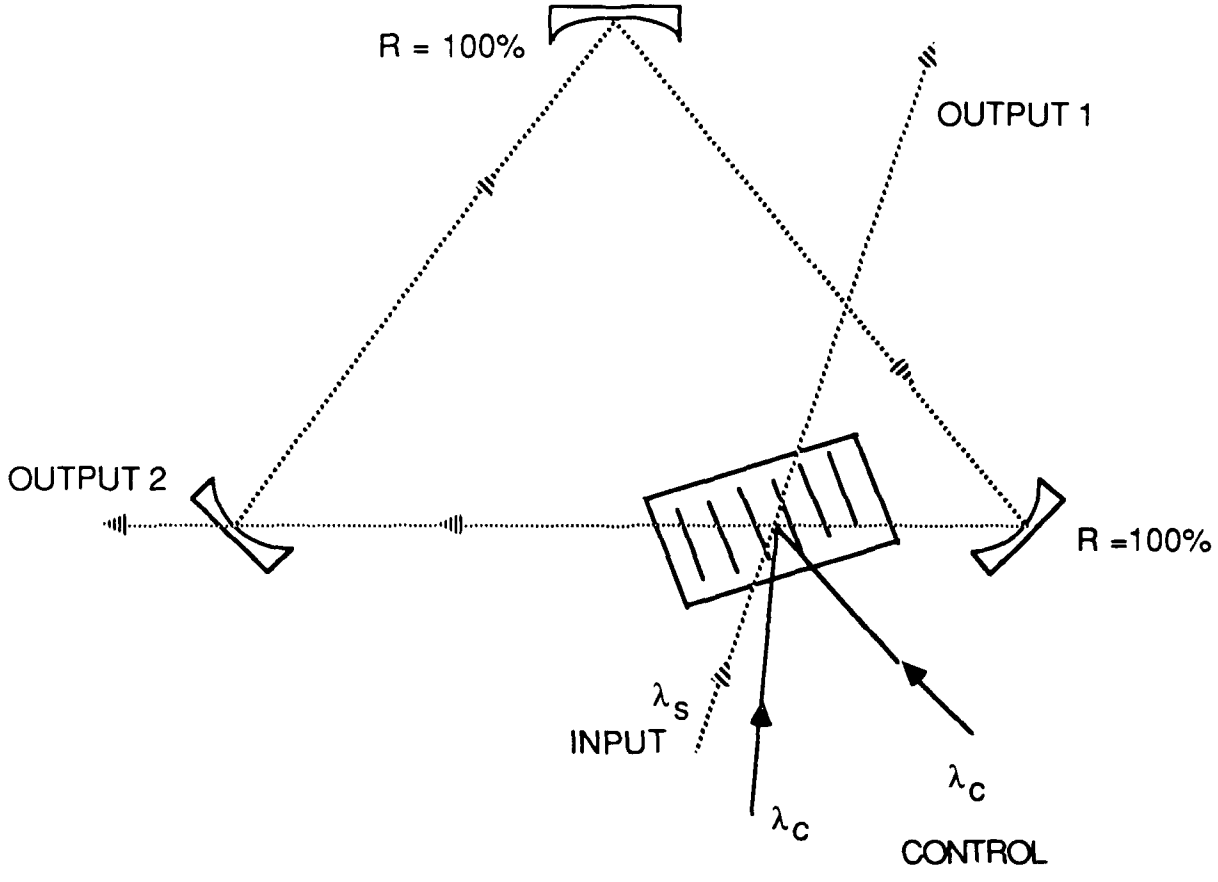

Figure 8. Ring cavity resonator. The dashed lines are the signal beam; solid lines are the signal.

END
DATE
FILMD
3-88
DTIC